

Improvement of MgO-C Bricks for BOF Based on Microstructure Investigation

Atsuhisa IIDA*¹Masayoshi KAKIHARA*²Minoru SUTO*³Hidenori TADA*⁴

Abstract

The recent development of our MgO-C brick technology which focuses on controlling the microstructure allows a wide extension of the variations in our product line up. It enables detailed optimization of brick arrangement corresponding to individually varied requirements. In this article, newly developed microstructure controlling technologies adopted for novel MgO-C bricks are introduced followed by a description of recommendable BOF brick applications taking operational condition into account.

1. Introduction

MgO-C brick is a composite comprised of MgO, which exhibits superior corrosion resistance against high basicity slag, and graphite, which has high thermal conductivity and poor wettability to molten slag. According to its excellent characteristics, MgO-C brick is widely used for steel refining vessels as a basic oxygen furnace (BOF), electric arc furnace (EAF), slag zone of steel ladle, and so on.

The first application of MgO-C brick for BOFs was implemented at Kawasaki Steel corporation (JFE Steel corporation at present) as a bottom blown tuyere of Q-BOP¹⁾⁻²⁾. While burnt dolomite bricks, which had been used for the BOF lining, were seriously damaged by cracking and peeling-off, applications of MgO-C drastically improved those damage factors. Thus, MgO-C brick had been rapidly substituted for dolomite bricks³⁾⁻⁵⁾. As a result, the main wear factor of BOF bricks has changed from spalling to slag corrosion.

Although slag corrosion is the main wear factor, there are other important wear factors for the BOF MgO-C brick depending on its application area. For instance, increase of heavy scrap charging causes abrasion wear at the impact area. In the case of the bottom tuyere, thermal spalling is still the main wear factor even through

MgO-C brick have excellent thermal shock resistance⁶⁾. Although gas decarburization (oxidation) is suppressed by sufficiently high partial pressure of CO gas on the whole, it occurs and promotes the wear of areas at which air tends to be mixed.

It is widely accepted that properties of MgO-C brick strongly depend on graphite fraction, purity of raw materials and arrangement of additives such as metallic powders. Adding to these compositional factors which can be evaluated numerically, the microstructure of MgO-C bricks, such as distribution and/or bonding status of grains, also affects material properties.

For approximately 20 years from late 1970s, when we began to manufacture MgO-C bricks, we developed various grades of MgO-C bricks by mainly optimizing the compositional factors. The developed products were successfully used, hence MgO-C brick technology for the BOF was regarded as having been established at that time. After another 20 years, however, we further improved the MgO-C bricks by focusing on microstructure control. As a result, various types of MgO-C materials specialized for individual application zones and operating conditions have been developed and contribute to the stable operation of the BOFs.

Typical microstructure controlling technologies are described as follows.

*¹ General Manager, Shaped Refractories R&D Sec., Research Center

*² Manager, Overseas Business Department for Americas, Europe/Middle East & Oceania

*³ General Manager, Manufacturing Sec. No.1, Okayama Plant, West Japan Works

*⁴ Executive Manager, Refractories Div., Ceratechno Co., Ltd.

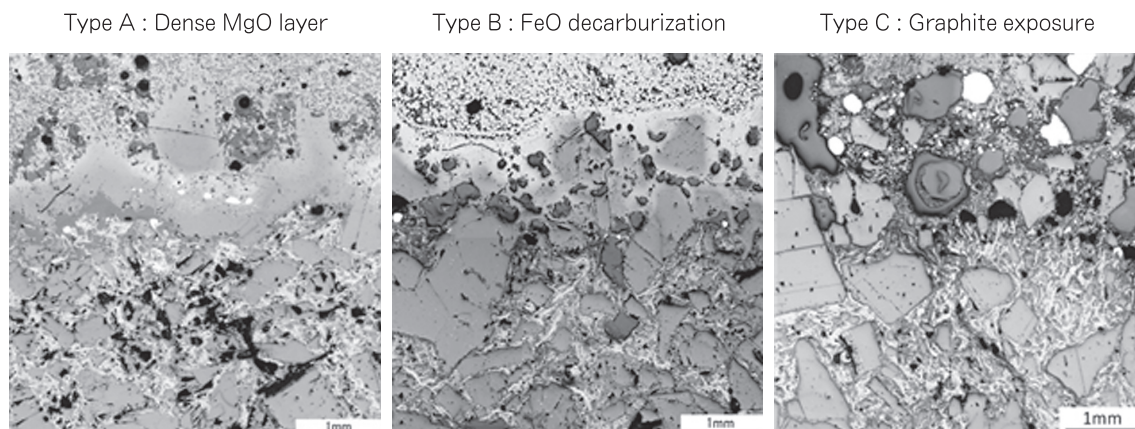


Fig.1 Three types of MgO-C brick hot face microstructures.

2. Microstructure Controlling Technologies for MgO-C Bricks

2.1 Improvement of slag corrosion resistance by inhibition of microstructure deterioration

It is well known that MgO-C brick corrosion resistance strongly depends on raw materials purity. When we observed the microstructure of post corrosion test specimens, particularly in the case of the rotary slag test, a dense MgO layer formation in the vicinity of the corroded surface was often recognized as shown in Fig.1A. Although the dense layer is composed of periclase crystals, it is accompanied by a boundary layer in which impurities of MgO and graphite are concentrated. Because the corrosion rate of the specimen depends on that of this newly formed layer, it is easy to understand that the corrosion resistance in laboratory tests strongly depends on raw material purity and is nearly independent of microstructure.

However, the dense MgO layer is seldom observed in the used bricks obtained from commercially operated BOFs. The common microstructures of MgO-C brick used in BOFs are shown in Fig.1B and 1C. The former is characterized by protrusion of MgO grain resulting from graphite oxidization by the FeO in the molten slag, and the latter shows protrusion of MgO grains coupled with graphite matrix exposure to slag. In addition, a slight gap formation between MgO grain and graphite was often observed in the microstructure of used bricks. These observations suggest that a microstructure including a loosened structure caused by gap formation also plays an important role in the BOF of wear mechanism.

Umeda et al⁷⁾ focused on the difference in porosity and strength of MgO-C brick between the values evaluated after heating at 1000°C, which are often used to show the typical qualities of the material, and the values evaluated for used brick obtained from an actual BOF. As a result, it was found that used bricks tend to exhibit higher porosity and lower strength than heat-treated specimens at 1000°C. Based on the hypothesis that the thermal fluctuation of commercial operations deteriorates the microstructure of MgO-C brick, they carried out a corrosion test for specimens that had been repeatedly heated prior to the corrosion test. As a result, the deteriorated microstructure was simulated by repeated laboratory heating and the microstructure-deteriorated specimen

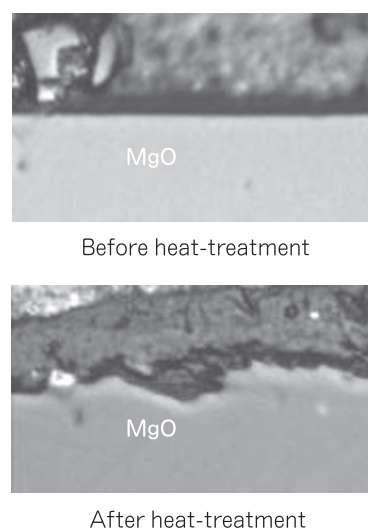


Fig.2 MgO grain boundary before and after heating.

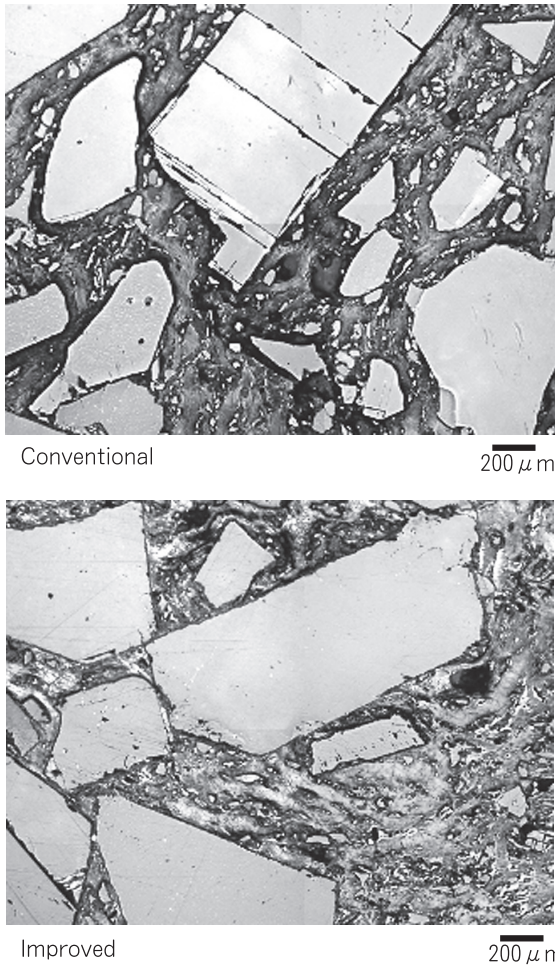


Fig.3 Comparison of microstructure between conventional and improved MgO-C brick after heating at 1500°C under reducing atmosphere.

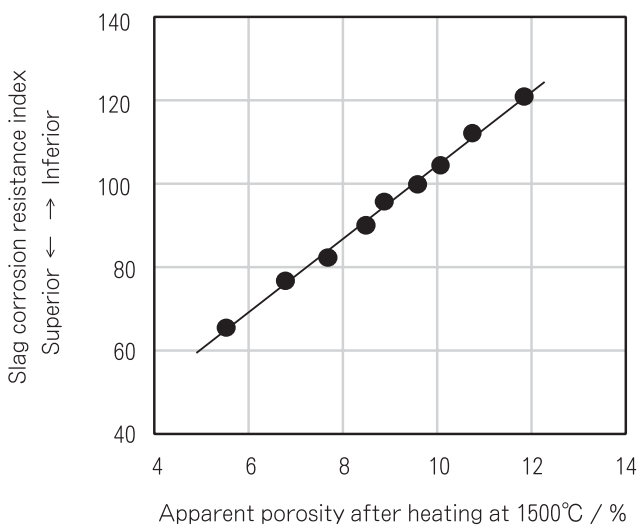


Fig.4 Variations in slag corrosion index as a function of apparent porosity after firing at 1500°C under reducing atmosphere.

showed considerable increase in slag corrosion rate.

Therefore, adding to purity of raw materials and the mixing formulation adjustment, it is important to suppress microstructure deterioration induced by long-term cyclic thermal fluctuation for improving the corrosion resistance in actual BOFs. Fig.2 shows the microstructure of grain boundary of MgO in MgO-C bricks before and after heating. The rough surface of the MgO grains in the post heated specimen is evidence of Mg gas evaporation as a result of the reaction between MgO grain and graphite. In other words, the evaporation of Mg promotes microstructure deterioration of MgO-C brick. According to detailed investigations, Carniglia[®] concluded that the rate-determining step of the reaction between MgO and C is the diffusion process of the Mg(g) and CO(g) out of the pore-channel structure of the brick. Therefore, densification of the microstructure suppresses the diffusion of the gases, resulting in suppression of the reaction. From this viewpoint, we optimized the grain size arrangement and manufacturing process in order to achieve a densified microstructure. Consequently, the microstructure deterioration caused by thermal fluctuation was successfully suppressed. The difference in microstructure after heating at 1500°C for a long time between conventional and improved MgO-C brick is demonstrated in Fig.3. Obviously, the reactions between the MgO grains and graphite matrix were suppressed in the improved material with a dense microstructure.

The influence of the microstructure deterioration on corrosion resistance was experimentally evaluated by a slag corrosion test performed for post heated microstructure-controlled MgO-C brick samples, which had the same proportion of MgO and graphite and the same raw material purity. Fig.4 shows the result. The specimens showed a wide range of porosity after heat treatment. And the low porosity specimen with the improved microstructure showed superior slag corrosion resistance.

2.2 Protection of working surface by promotion of slag coating

It is well known that a slag coating on the working surface protects against MgO-C brick wear in the BOF. Because the slag coating inhibits the reaction between MgO and graphite due to the high internal Mg and CO gas pressure, it also suppresses microstructure deterioration. Although development of the slag coating strongly depends on the BOF operation process, the microstructure

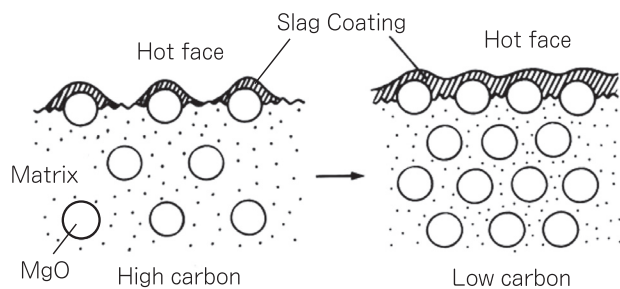


Fig.5 Conceptual image of hot face protection by slag coating.

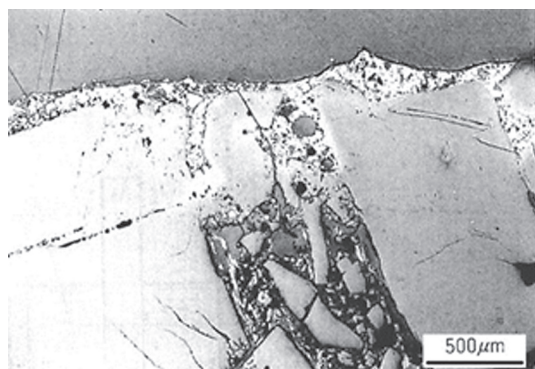


Fig.6 Microphotograph of hot face of improved material after use.

of MgO-C bricks also affects the development of the slag coating.

Fig.5 shows a conceptual image of the relationship between the microstructure and formation of slag coating layer. Because slag adheres to only MgO grains exposed to the hot surface, increasing the MgO surface area in the vicinity of the hot surface is important to promote slag coating. Although application of fine MgO grain seems to increase the MgO surface area, the fine MgO grains easily dissolve into the slag and do not remain on the hot surface. Therefore, we optimized the grain size distribution of MgO to promote the coating. Fig.6 shows an example of the microstructure of improved MgO-C brick which shows the formation of the slag coating.

2.3 Microstructure reinforcement by evaporation-condensation effect of pitch

As generally accepted, metallic additives effectively enhance the strength of resin bonded MgO-C bricks. However, since metallic additives become effective only at high temperatures, they tend to cause considerable difference in Young's modulus between the high temperature working surface and the intermediate temperature middle

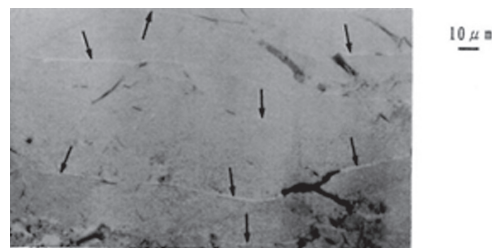


Fig.7 Pitch filling state in interstices among graphite layers.

area of brick lining, which is a negative status in terms of thermal spalling. Another approach to reinforcing the microstructure is carbon bond enhancement by pitch addition. This approach is effective in the intermediate temperature range and also effective in decreasing Young's modulus of the brick, both of which improve thermal spalling resistance.

Carbon bond enhancement is achieved through the evaporation and condensation effect of pitch. Fig.7 shows an example of a laboratory test for the evaporation-condensation effect of pitch⁹. The specimen was prepared by pressing the mixture of flake graphite and pitch. After heating at 800°C the microstructure was observed. Arrows indicate the pitch-derived condensed carbon that fills the fine interstices of graphite flake.

2.4 Microstructure reinforcement by whisker formation

The charging side of the BOF is worn by mechanical abrasion caused by scrap charging. In general, increase of hot strength by metallic additives is an effective measure against this type of wear. However, since an increase in metallic additives tends to lower spalling resistance, improvement of the abrasion resistance should be achieved by using the minimum quantity of metallic additives. It is well known that metal additives in MgO-C brick show various types of behavior such as melting, carbidation, nitridation, and oxidation. The behavior depends on not only temperature and atmosphere but also distribution of the additives. Hence, it is important to achieve the microstructure that efficiently utilizes the behavior of metallic additives under the conditions of BOF operation.

Fig.8 shows the hot modulus of ruptures of two kinds of MgO-C bricks including the equivalent amount of the same kinds of metal. Improved material shows higher hot strength due to optimized particle size and dispersion

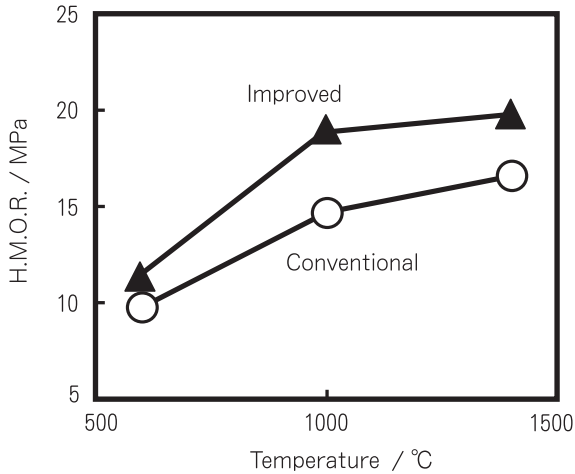


Fig.8 Influence of metal distribution configuration in MgO-C brick on H.M.O.R..

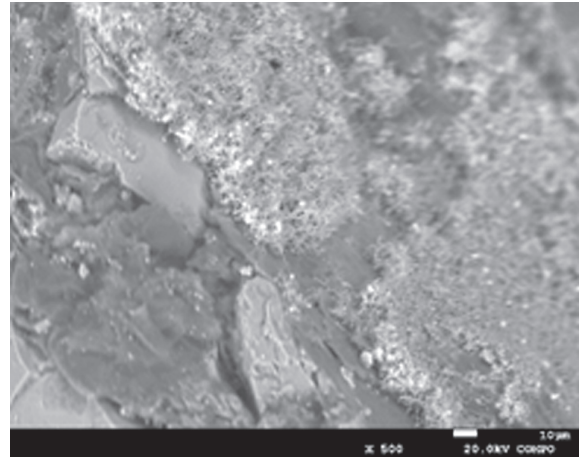


Fig.9 Microstructure of fracture surface of improved MgO-C brick after bending test.

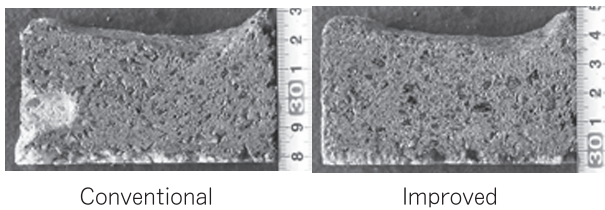


Fig.10 Cross sections of MgO-C bricks after hot abrasion test.

of the metal additives. As shown in Fig.9, the improved material is characterized by a homogeneously distributed whisker formation on its fractured surface after the bending test. Fig.10 is cross sections of the specimens after the hot abrasion test, which materials are identical to those shown in Fig.8. The improved material with a 20% increase in hot strength showed 15% decrease in abrasion volume.

2.5 Inhibition of crack propagations by increase in fracture toughness

As is well known, spalling resistance of refractory material consists of resistance against crack initiation and resistance against crack propagation. There are some areas where the latter resistance is important.

Fig.11 shows load-displacement curves of typical MgO-C bricks obtained by three point bending test. Specimens were heated at 1200°C prior to the fracture evaluation. The initial slope of the curve, that is the increase in degree of load as a function of displacement, is equivalent to static elasticity. The maximum load point and subsequent load relaxation behavior express crack initiation and crack

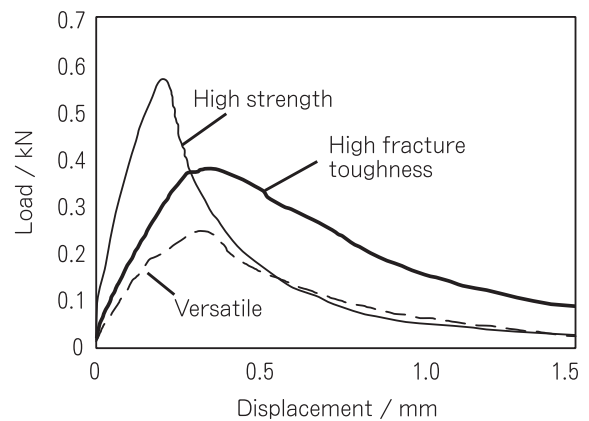


Fig.11 Load-displacement curves of several kinds of MgO-C bricks after firing at 1200°C

propagation, respectively. Since MgO-C brick contains a large amount of flat shaped flake graphite, crack propagation resistance is larger than ordinal oxide bricks. Thus, MgO-C bricks show gradual decrease of the load after cracking while ordinal oxide bricks show brittle behavior characterized by abrupt decrease of the load. The integral of the curve in the crack propagation stage corresponds to the work of fracture consumed for the crack propagation. High fracture toughness material exhibits large work of fracture at the crack propagation stage. Generally, addition of metallic additives increases strength but does not increase the fracture toughness of MgO-C brick. Hence, another microstructure controlling technology is necessary for improving the crack stability coefficient (R_{st}), which expresses crack propagation resistance.

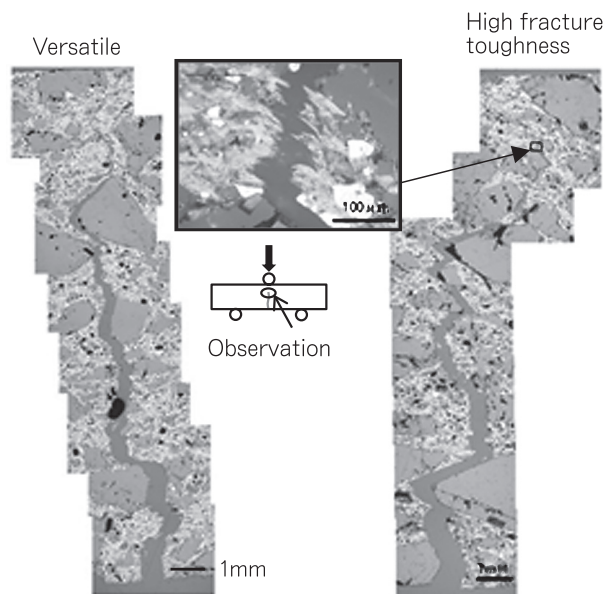


Fig.12 Crack propagation path observed in MgO-C bricks after bending test.

Fig.12 shows the crack propagation path observed in post bending test specimens. High fracture toughness material showed large zigzag deviation of the crack propagation path. Fig.13 is a microphotograph of the fracture surface of this material. The presence of protruding graphite shapes suggests the pulling-out prevention effect, which increases crack propagation resistance.

3. Variations of MgO-C Bricks for BOF

We can commercially provide various types of MgO-C bricks with unique properties utilizing the microstructure control technology described above.

The typical properties of 5 kinds of materials are listed in Table 1. Material A is a standard MgO-C brick for

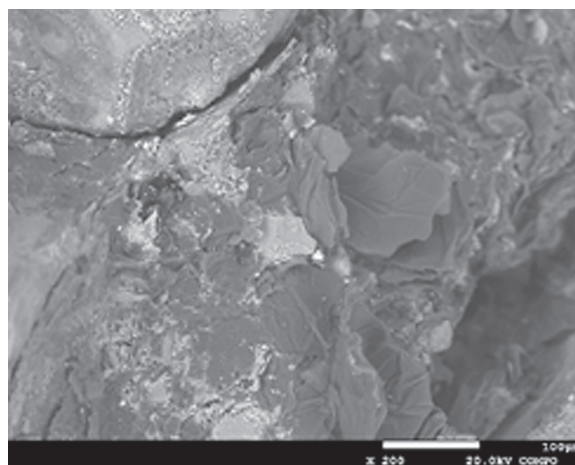


Fig.13 Microstructure of fracture surface of high fracture toughness MgO-C brick after bending test.

general use. The high versatility of this product allows various kinds of applications including the bottom and metal bath of the BOF. Material B, which is specialized for chemical corrosion resistance, is suitable for high corrosive areas such as the slag line of the BOF, hot spot of the EAF, slag line of the steel ladle, and so on. High strength material C places importance on mechanical abrasion resistance. Material D, containing a larger amount of graphite, focuses on suppressing cracking and peeling-off. Low carbon material E is characterized by resistance against erosion derived from graphite oxidation.

The apparent porosities of the products, after being heated at 1000°C and 1500°C, are compared in Fig.14. Material B shows the lowest porosity for both heating temperatures among the 5 materials. The apparent porosity of this material is only 7% even when heated to 1500°C. Low carbon material E also maintains a low porosity of

Table 1 Material properties for BOF bricks

Material	A	B	C	D	E
Chemical composition / mass%					
MgO	78	78	76	67	84
C	17	17	16	30	10
Typical properties					
Bulk Density / g·cm ⁻¹	2.95	3.06	2.98	2.71	3.08
Cold crushing strength / MPa	36	31	49	38	53
Remarks	General versatility	Corrosion resistance	Abrasion resistance	Fracture toughness	Oxidation resistance

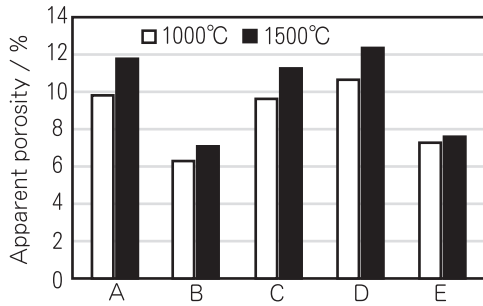


Fig.14 Apparent porosity of MgO-C bricks after firing at 1000°C and 1500°C.

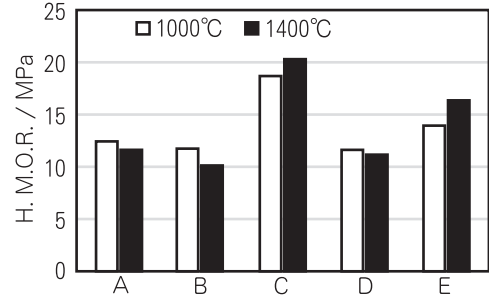


Fig.15 H.M.O.R of MgO-C at 1000°C and 1400°C.

8% after being heated to 1500°C. Because of a larger amount of metallic additives, material C showed a higher porosity increase after 1500°C heating than materials B and E. However, the porosity increase is suppressed to a lower percentage than standard materials by optimizing the particle size and distribution of metallic additives.

Materials C and E showed higher hot strength at 1000 and 1400°C as shown in Fig.15. Thanks to the dispersion technology of particle size-optimized metallic additives, a sufficient increase in hot strength was achieved by minimizing the amount of metallic additives in these materials.

4. Wear Mechanism of Each BOF Area and Suitable Material

Fig.16 shows a typical refractory lining of a BOF. In order to deal with the wear mechanism of each area, several kinds of MgO-C bricks are applied. The effect of such application is briefly summarized in Table 2.

4.1 Upper cone

At the upper cone of the BOF, slag corrosion or peeling-off are not significant wear factors due to skull adhesion. On the other hand, the influence of air oxidation is not negligible. Particularly at the area around the mouth, microstructure deterioration tends to occur through gas decarburization. Therefore, the material A including larger amount of antioxidants are applied.

On the other hand, slag corrosion also should be taken into account at the area around the tapping hole where refractories are exposed to a sufficient amount of molten slag at the final stage of tapping. In rare cases, slag corrosion at the boundary area between the upper cone and barrel occurs as a result of an inadequate height arrangement of the oxygen blowing lance. In these cases, material B, with excellent slag corrosion resistance, is suitable.

4.2 Barrel

Slag corrosion is the most important wear factor for refractories lined in the barrel of the BOF. This is

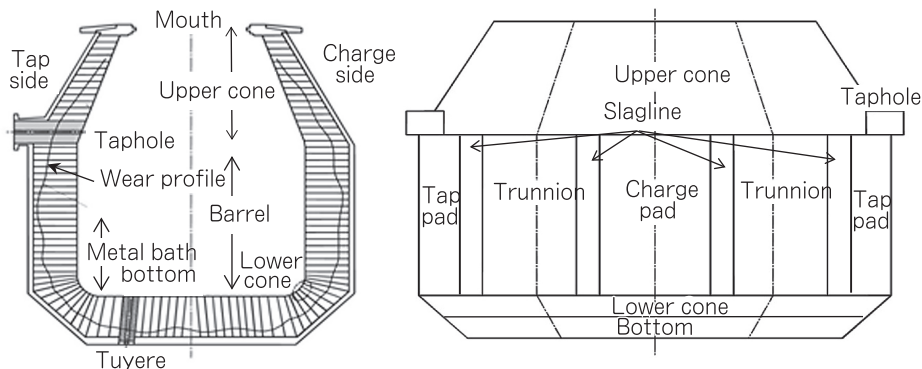


Fig.16 Typical zoned lining for BOF and industrial terms for each zone.

Table 2 Optimal BOF lining recommendations

		Material	Wear rate mm/heats	Improved degree
Upper cone	Ordinal part	A	0.09	10%
	Corrosive part	B	0.06	25%
Barrel	Ordinal part	A	0.11	10%
	Slag line, Trunnion	B	0.19	25%
	Charge pad with intensive abrasion	C	0.23	20%
	Charge pad without intensive abrasion	B	0.19	20%
Lower cone	Metal bath	A	0.14	10%
Bottom	Ordinal part	A	0.12	10%
	Tuyere	D	0.45	20%
Tapping hole sleeve		E	0.17	20%

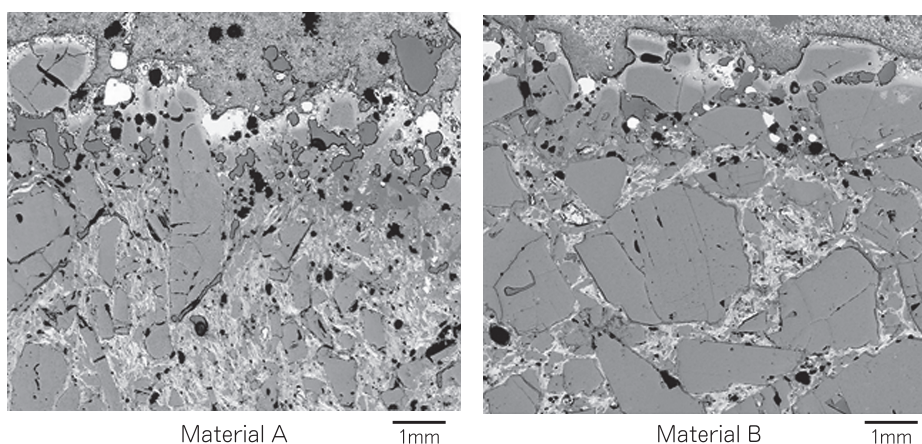


Fig.17 Comparison of hot face microphotographs between Materials A and B after use.

pronounced in two critical wear areas such as; the slag line levels (slag line of the blowing stage and that of the tapping stage) and the trunnion side where both slag coating and hot repairing are difficult. In those areas, corrosion by microstructure deterioration is considerably accelerated. Thus, material B, with the high deterioration resistance, is strongly recommended. Fig.17 shows the microstructures of materials A and B used at the tapping side of the barrel. Both the deterioration thickness and gap width between the MgO grains and graphite matrix of material B are smaller than those of material A

In the case of the charge pad area of the barrel (Fig.18), abrasion caused by mechanical shock due to scrap charging is also a dominant wear factor. Material C, with high

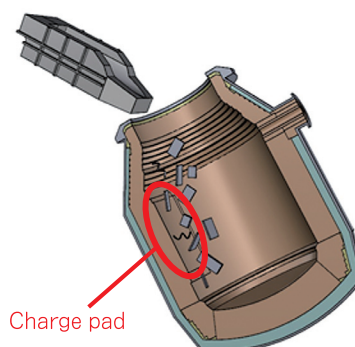


Fig.18 Schematic illustration of scrap impact damage of BOF charge pad.

strength, is suitable for this area. However, abrasion wear is a complex phenomenon accompanied by cracking, the wear rate is strongly affected by the amount, shape and size of the scraps. There are cases where the application of material B is effective for this area depending on the kinds of charged scrap.

As is widely adopted in North America, splash coating, where slag is intentionally adhered to the BOF working surface utilizing oxygen lance is effective for preventing BOF lining wear. In that case, versatile material A is applicable.

4. 3 Steel bath and bottom

Mechanical abrasion caused by heavy scraps occurs in not only the charge pad area but also the steel bath and

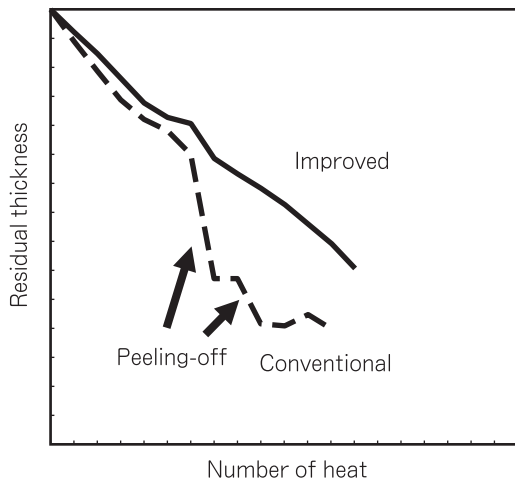


Fig.19 Comparison of reduction trend in residual thickness of tuyere MgO-C Bricks between conventional and improved.

bottom area. However, the wear rate of the steel bath and bottom area is relatively small so that versatile material A or lower grade materials can be applied.

However, the bottom blown tuyeres are highly worn areas, which affects the blowing operation. The bottom blown tuyeres are functional refractories essential for improvement of smelting efficiency and/or metallurgical properties. There are several types of tuyere so a suitable blowing method is selected depending on BOF operating conditions; the multi hole plug (MHP), which blows inert gas as argon through a lot of small pipes arranged in MgO-C brick, the double tube through which oxygen and hydrocarbonaceous gas are blown, and so on. In all types, increase of blowing-gas volume promotes the wear rate of the bottom tuyeres, resulting in a critical wear area affecting the service life of the BOF. Performance of tuyere brick is markedly shortened by discontinuous reduction in residual thickness, which is caused by repeatedly occurring thick peeling-off resulting from crack propagation at the inner part of the brick. Hence, material D, with high fracture toughness, is recommended for the tuyere brick in terms of crack propagation resistance. Fig.19 shows the changes in residual thickness of the tuyere brick. Compared with conventional material, frequently showing discontinuous thickness change induced by peeling-off, material D type showed stable change in residual thickness, resulting in considerable reduction in the wear rate.

4. 4 Tapping hole

Fig.20 shows a schematic image of a tapping hole. The tapping hole is the path through which refined steel flows

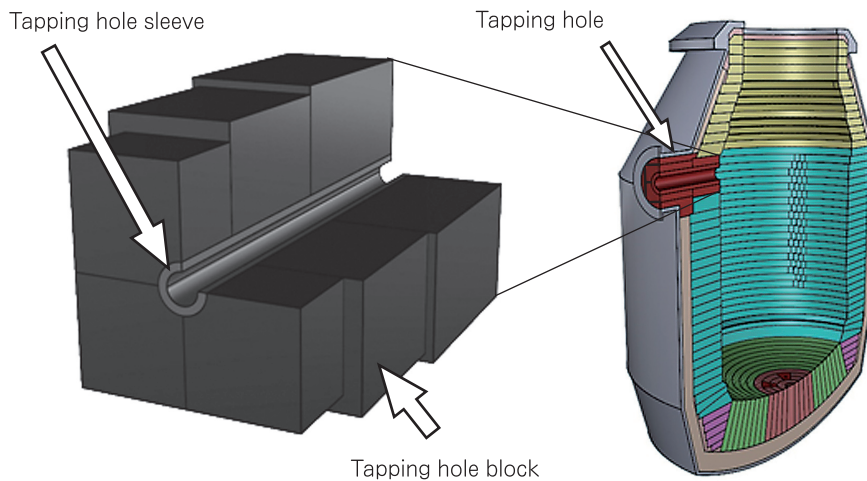


Fig.20 Schematic illustration of BOF tapping hole sleeve and block.

during discharging into the steel ladle. In view of preventing molten steel leakage, applications of large blocks for the tapping hole lining have been extending to reduce the number of joint. Since molten steel is drained through the tapping hole sleeve, which is an exchangeable pipe-shape brick inserted in the tapping hole, versatile material A is applied for the tapping hole blocks.

On the other hand, the tapping hole sleeve is one of the important parts in terms of stable high availability BOF operation. Since graphite oxidation deteriorates microstructure in this part, application of low carbon MgO-C material is desirable in terms of abrasion resistance. On the other hand, thermal spalling resistance is also necessary for the tapping hole sleeve. We recommend material

E, which is a low carbon material but has sufficient spalling resistance due to optimized grain size distribution and microstructure control.

5. Conclusions

We developed various kinds of MgO-C brick based on microstructure control investigations. Improvements in slag corrosion resistance, abrasion resistance, spalling resistance and so on were realized with individually optimized microstructures. These distinctive MgO-C bricks are being successfully applied to commercial BOF operations. We will continue to develop our products to sustain progress in the high temperature industry.

References

- 1) R. Uchimura, M. Kumagai, T. Morimoto, S. Harita : Taikabutsu, **31** [6] 285-295 (1979).
- 2) T. Morimoto, S. Harita : Taikabutsu, **31** [9] 440-445 (1979)
- 3) T. Morimoto, S. Harita : Taikabutsu, **32** [3] 141-144 (1980).
- 4) K. Enami, N. Yoshino, H. Kyouda, H. Nishio: Taikabutsu, **32** [3] 144-148 (1980).
- 5) T. Kouno, A. Tabata: Taikabutsu, **32** [3] 163-169 (1980).
- 6) T. Kashiwa, Y. Kitano, H. Nishikawa, S. Hosohara, S. Nabeshima, M. Okuno: CAMP-ISIJ, **16** 118 (2003).
- 7) S. Umeda, T. Ikemoto, T. Matsui: Taikabutsu, **59** [10] 544-551 (2007).
- 8) S. C. Carniglia : Am. Cer. Soc. Bul., **52** [2] 160-165 (1973).
- 9) Y. Hoshiyama, O. Nomura, H. Nishio, K. Ichikawa: Taikabutsu, **48** [1] 35-41 (1996).